14th International Symposium on Turbulence and Shear Flow Phenomena (TSFP14)
Heidelberg, Germany, July 28-31, 2026

ANALYSIS OF DYNAMO EFFECT IN MHD TURBULENT CHANNEL FLOW

Pinzhong Yang
Institute of Industrial Science
University of Tokyo
Komaba, Meguro-ku, Tokyo 153-8505, Japan
pinzhong@iis.u-tokyo.ac.jp

Fujihiro Hamba
Institute of Industrial Science
University of Tokyo
Komaba, Meguro-ku, Tokyo 153-8505, Japan
hamba@iis.u-tokyo.ac.jp

ABSTRACT

In some magnetohydrodynamic (MHD) turbulent flows, turbulent motion can generate and sustain large-scale magnetic fields against the diffusion effect. It is called the turbulent dynamo effect (Krause and Radler, 1980). The α effect represents the component of the turbulent electromotive force that is proportional to the mean magnetic field, has been a typical dynamo effect that explains the generation and sustainment of large-scale magnetic fields in astrophysical systems such as stars, galaxies, and planets (Moffatt, 1978; Parker, 1979). In addition, other dynamo effects have also been proposed and examined such as the cross-helicity effect, which contributes to the turbulent electromotive force through a term proportional to the mean vorticity (Yoshizawa, 1990; Yokoi, 2023).

Hamba and Tsuchiya (2010) carried out a large eddy simulation (LES) of MHD turbulent channel flow to investigate the dynamo effects. They evaluated the production terms in the transport equation for the turbulent electromotive force and demonstrated the importance of the cross-helicity effect. However, it was not clear whether the results are accurate enough because a subgrid-scale model was used in the LES. The pumping effect, which corresponds to the transport of the mean magnetic field by turbulence, was not investigated.

In the present study, we carried out a direct numerical simulation (DNS) of MHD turbulent channel flow to obtain accurate numerical results without using a subgrid-scale model. Similar to Hamba and Tsuchiya (2010), we evaluated the transport equation for the turbulent electromotive force. We related the production terms to terms in its model expression including the cross-helicity effect and the pumping effect. We clarified the mechanism of the generation and sustainment of the large-scale mean magnetic field in the present MHD flow.

NUMERICAL METHOD

In the present simulation we solve the incompressible MHD equations in Alfvén units using a finite difference method. The Navier-Stokes and continuity equations for the velocity of incompressible MHD flow are given by

$$\frac{\partial \boldsymbol{u}}{\partial t} = -(\boldsymbol{u}\cdot\boldsymbol{\nabla})\mathbf{u} + (\boldsymbol{b}\cdot\boldsymbol{\nabla})\mathbf{b} - \boldsymbol{\nabla} p_M + \upsilon \boldsymbol{\nabla}^2 \boldsymbol{u} \quad (1)$$

$$\boldsymbol{\nabla}\cdot\boldsymbol{u} = 0 \quad (2)$$

where $\boldsymbol{u}$ is the velocity, $\boldsymbol{b}$ is the magnetic field, $p_M(= p/\rho + \boldsymbol{b}^2/2)$ is the MHD pressure, υ is the viscosity. The magnetic field $\boldsymbol{b}$ follows the induction equation and solenoidal condition which are given by

$$\frac{\partial \boldsymbol{b}}{\partial t} = -\boldsymbol{\nabla}\times\boldsymbol{e}, \quad \boldsymbol{e} = -\boldsymbol{u}\times\boldsymbol{b} + \lambda_M \boldsymbol{j} \quad (3)$$

$$\boldsymbol{\nabla}\cdot\boldsymbol{b} = 0 \quad (4)$$

where $\boldsymbol{e}$ is the electric field, $\boldsymbol{j}(= \boldsymbol{\nabla}\times\boldsymbol{b})$ is the electric current density, λ_M is the magnetic diffusivity. We adopt Alfvén velocity units in the present paper.

The computation domain is $L_x \times L_y \times L_z = 4\pi \times 2 \times \pi$ and the grid number is $N_x \times N_y \times N_z = 256 \times 90 \times 128$, where x, y, and z denote the streamwise, wall-normal, and spanwise directions. A uniform grid is used in the streamwise and spanwise directions, and a non-uniform grid is used in the wall-normal direction to resolve the near-wall region. The flows are driven by a constant external pressure gradient in streamwise direction. The length scale is normalized by the channel half width $L_y/2$, whereas the velocity and the magnetic fields are normalized by the friction velocity u_τ. The Reynolds number and magnetic Reynolds number defined by friction velocity are set as $Re_\tau = Rm_\tau = 180$. Periodic boundary conditions are imposed in the x and z directions, while no-slip and insulating conditions are applied at boundary at $y = \pm 1$.

TURBULENCE MODELING

To investigate the large-scale mean magnetic field generation and the turbulent dynamo mechanisms in MHD, we decompose the variables into mean and fluctuating components to derive the corresponding mean-field equations. The induction equation for the mean magnetic field $\boldsymbol{B}$ is given by

$$\frac{\partial \boldsymbol{B}}{\partial t} = \boldsymbol{\nabla}\times(\boldsymbol{U}\times\boldsymbol{B}) + \boldsymbol{\nabla}\times\boldsymbol{E}_M + \lambda_M \nabla^2 \boldsymbol{B} \quad (5)$$

where $\boldsymbol{B}(= \langle \boldsymbol{b} \rangle)$ is the mean magnetic field in Alfvén speed units, $\boldsymbol{U}(= \langle \boldsymbol{u} \rangle)$ is the mean velocity, and λ_M is the magnetic diffusivity. The turbulent electromotive force $\boldsymbol{E}_M$ is defined as

$$\boldsymbol{E}_M = \langle \boldsymbol{u}' \times \boldsymbol{b}' \rangle \quad (6)$$

where $\boldsymbol{u}'$ and $\boldsymbol{b}'$ are the fluctuating velocity and magnetic field, respectively. It represents the turbulent effect in the mean magnetic field evolution. In order to close the system of

MHD equations, $\boldsymbol{E}_M$ needed to be modelled by the mean field and turbulent statistical quantities. In mean-field dynamo theory, a model equation for $\boldsymbol{E}_M$ is given by (Yoshizawa and Hamba, 1988; Yoshizawa, 1990; Yokoi, 2023)

$$\boldsymbol{E}_M = \alpha\boldsymbol{B} - \beta\boldsymbol{J} + \gamma\boldsymbol{\Omega} + \boldsymbol{u}_p \times \boldsymbol{B} \tag{7}$$

where $\boldsymbol{\Omega}(= \boldsymbol{\nabla} \times \boldsymbol{U})$ is the mean vorticity and $\boldsymbol{J}(= \boldsymbol{\nabla} \times \boldsymbol{B})$ is the mean electric current density. The first term on the RHS of (7) proportional to the mean magnetic field $\boldsymbol{B}$ means that the turbulent electromotive force is generated parallel or anti-parallel to the mean magnetic field, representing the α effect; The second term on the RHS of (7) is the turbulent diffusivity effect, representing that the turbulent motion enhances the diffusion effect of the mean magnetic field; The third term on the RHS of (7) proportional to the mean vorticity $\boldsymbol{\Omega}$ represents the cross-helicity effect, and the transport coefficient γ is expressed in term of the turbulent cross helicity $W(= \langle \boldsymbol{u}' \cdot \boldsymbol{b}' \rangle)$; The fourth term on the RHS of (7) is the pumping effect term, and $\boldsymbol{u}_p$ plays a role like the mean velocity and is called the pumping velocity.

RELATIONSHIP BETWEEN PRODUCTION TERMS OF $\boldsymbol{E}_M$ AND ITS MODEL EQUATION

The model terms of the turbulent electromotive force given by (7) are just a candidate for actual dynamo phenomena. Some model terms have not been examined well yet, and other dynamo mechanisms may also exist. Therefore, in the present work, we analyze the production terms of the transport equation for the turbulent electromotive force to investigate the turbulent dynamo effect, as this approach directly clarifies the generation mechanism of the turbulent electromotive force. The transport equation for the turbulent electromotive force and its production terms are given by

$$\frac{\partial E_{Mi}}{\partial t} = P_{emi} - \varepsilon_{emi} + \Pi_{emi} + \mathrm{D}_{emi} + \mathrm{T}_{emi} \tag{8}$$

$$P_{emi} = P_{\alpha i} + P_{\beta i} + P_{\gamma i} + P_{pi} + P_{\alpha si} \tag{9}$$

$$P_{\alpha i} = \frac{1}{3} H B_i \tag{10a}$$

$$P_{\beta i} = -\langle u_j' u_l' + b_j' b_l' \rangle \frac{\partial B_k}{\partial x_l} \epsilon_{ijk} \tag{10b}$$

$$P_{\gamma i} = \langle u_j' b_l' + b_j' u_l' \rangle \frac{\partial U_k}{\partial x_l} \epsilon_{ijk} \tag{10c}$$

$$P_{pi} = \{-(\boldsymbol{\nabla} \cdot \boldsymbol{K}_R) \times \boldsymbol{B}\}_i \tag{10d}$$

Here $P_{\alpha i}$, $P_{\beta i}$, $P_{\gamma i}$, P_{pi}, and $P_{\alpha si}$ are the production terms proportional to the mean field or the mean field gradient. The production term $P_{\alpha i}$ proportional to the mean magnetic field is related to the α effect; The production term $P_{\beta i}$ proportional to the mean magnetic field gradient is related to the turbulent diffusivity effect; The production term $P_{\gamma i}$ proportional to the mean velocity gradient and the cross correlation of the velocity and magnetic fluctuations is related to the cross-helicity effect; The production term P_{pi} written in the form of the cross product with the mean magnetic field is related to the pumping effect, and the pumping velocity $\boldsymbol{u}_p$ is considered proportional to the quantity $-(\boldsymbol{\nabla} \cdot \boldsymbol{K}_R)$, where $K_{Rij} = \langle u_i' u_j' - b_i' b_j' \rangle / 2$. The expression of $P_{\alpha si}$ is omitted here. In the present work, we directly evaluate these production terms to examine the related dynamo effects.

TIME HISTORY OF VOLUME-AVERAGED QUANTITIES

In the present DNS, a large-scale mean magnetic field is expected to be generated. First, we examine the time history of the volume-averaged magnetic field defined as

$$B_{xvol} = \frac{1}{L_x L_y L_z} \iiint b_x \, dxdydz \tag{11}$$

In Figure 1, after $t = 600$, B_{xvol} fluctuates around 2.4, indicating that a large-scale magnetic field is generated and a nearly steady state is achieved. Since no external electromotive force is applied, some dynamo mechanism must exist. Figure 2 shows the time history of the volume-averaged turbulent kinetic and the magnetic energy defined as

$$K_{uvol} = \frac{1}{L_x L_y L_z} \iiint (\boldsymbol{u} - \langle \boldsymbol{u} \rangle_{xz})^2 dxdydz \tag{12a}$$

$$K_{bvol} = \frac{1}{L_x L_y L_z} \iiint (\boldsymbol{b} - \langle \boldsymbol{b} \rangle_{xz})^2 dxdydz \tag{12b}$$

where $\langle \cdot \rangle_{xz}$ denotes the x-z plane average. After $t = 600$, the value of K_{uvol} increases to about 5 and the value of K_{bvol} decreases to about 1. The difference between K_{uvol} and K_{uvol} is clearly seen. This time period corresponds to the period when a large value of B_{xvol} is sustained in Figure 1. The time history of the volume-average quantities imply that a statistically steady state is achieved after $t = 600$ till $t = 1500$.

MEAN MAGNETIC FIELD AND SECOND ORDER STATISTICS

To investigate dynamo effects generating the large-scale magnetic field in Figure 1, we focus on the time period at $600 < t < 1500$. Hereafter, statistical quantities are obtained by taking averages over the x-z plane and over this time period.

Figure 3 shows the mean magnetic field B_x. It has a positive profile with a maximum value around the channel center at $y = 0$. The induction equation of B_x is given by

$$\frac{\partial B_x}{\partial t} = -\frac{\partial E_z}{\partial y} \tag{13}$$

$$-E_z = E_{Mz} - \lambda_M J_z \tag{14}$$

where $E_{Mz} = \langle u_x' b_y' - u_y' b_x' \rangle$. Figure 4 shows the terms in (14). The mean electric field E_z has a nearly constant value about -0.003 that suggests that B_x reached a nearly steady state. The Ohmic term $-\lambda_M J_z$ shows a negative gradient in the core region at $-0.9 < y < 0.9$, producing a negative value on the RHS of (13). It represents the diffusion effect which decreases B_x over time. In contrast, the turbulent electromotive force E_{Mz} has a positive gradient, producing a positive value on the RHS of (13). It represents the turbulent dynamo effect which increases B_x over time in the core region.

Figures 5-7 show the profiles of the three components of the root mean square (RMS) of the velocity fluctuations, the RMS of the magnetic field fluctuation, and the turbulent cross helicity $W_{\alpha\alpha}(=\langle u'_\alpha b'_\alpha \rangle)$, respectively. These figures also reflect the turbulent kinetic energies $K_{u\alpha\alpha}(=\langle u'^2_\alpha \rangle/2)$, the turbulent magnetic energies $K_{b\alpha\alpha}(=\langle b'^2_\alpha \rangle/2)$, and the cross-correlation between the velocity and magnetic field fluctuations, respectively. Here α represents x, y, and z. In Figure 5, $\langle u'^2_x \rangle^{1/2}$ is nearly twice as large as that in the non-MHD case, because the turbulent kinetic energy is produced by the mean velocity gradient which is larger in the MHD case. On the other hand, both $\langle u'^2_y \rangle^{1/2}$ and $\langle u'^2_z \rangle^{1/2}$ are smaller than that in the non-MHD case. Therefore, the anisotropy of the turbulent kinetic energy in the MHD case is stronger than that in the non-MHD case, and the turbulent magnetic energy and turbulent cross helicity also exhibit this strong anisotropy. In Figure 6, the RMS of the magnetic field fluctuation is smaller than that of the velocity fluctuation as shown in Figure 5, which is consistent with the observation that the turbulent magnetic energy is smaller than the turbulent kinetic energy as shown in Figure 2. The turbulent kinetic and magnetic energies exhibit similar profiles, with peak values in the near-wall region and a gradual decrease toward the channel center. In Figure 7, the turbulent cross helicity takes positive values, except that W_{xx} is negative in the near-wall region.

GENERATION OF E_{Mz}

The transport equation for the turbulent electromotive force E_{Mz} and its production terms are given by

$$\frac{\partial E_{Mz}}{\partial t} = P_{emz} + \Pi_{emz} - \varepsilon_{emz} + \mathrm{D}_{emz} + \mathrm{T}_{emz} \tag{15}$$

$$P_{emz} = P_{\beta z} + P_{\gamma z} + P_{pz} + P_{\alpha sz} \tag{16}$$

$$P_{\beta z} = \langle u'^2_y + b'^2_y \rangle \frac{\partial B_x}{\partial y} \tag{17a}$$

$$P_{\gamma z} = -2\langle u'_y b'_y \rangle \frac{\partial U_x}{\partial y} \tag{17b}$$

$$P_{pz} = \frac{\partial K_{Ryy}}{\partial y} B_x \tag{17c}$$

Here, $P_{\beta z}$, $P_{\gamma z}$, P_{pz}, and $P_{\alpha sz}$ are the production terms related to the mean field quantities. Figure 8 shows the terms on the RHS of (16). Because the mean magnetic field B_z has a negligible small value, there is no α effect in the present flow, and $P_{\alpha z}$ was omitted.

According to (7) and (10), the production term $P_{\beta z}$ proportional to the mean magnetic field gradient is related to the turbulent diffusivity effect, and it shows opposite sign to that of the turbulent electromotive force, which means the loss of E_{Mz}. Therefore, the turbulent diffusivity plays a role of the diffusion effect of the mean magnetic field.

The production term $P_{\gamma z}$ proportioanl to the mean vorticity Ω_z and the cross-helicity $W_{yy}(=\langle u'_y b'_y \rangle)$ is related to the cross-helicity effect. It shows the same sign as that of the turbulent electromotive force, representing the generation of E_{Mz}. Therefore, the cross-helicity plays a role of the dynamo effetct in the channel flow. At the meanwhile, $P_{\gamma z}$ has the largest magnitude among the production terms, and it is the domoinant dynamo effect in the present MHD channel flow.

The production term P_{pz} is related to the pumping effect. In the core region at $-0.75 < y < 0.75$, P_{pz} shows the same sign as that of the turbulent electromotive force, representing the generation of E_{Mz}. Therefore, the pumping effect plays a role of the dynamo effetct in the core region at $-0.75 < y < 0.75$ in the present channel flow.

The exact expressions and discussions of the production term $P_{\alpha\alpha z}$, the pressure-strain correlation term Π_{emz}, the dissipation term $-\varepsilon_{emz}$, the diffusion term D_{emz}, and the triple correlation term T_{emz} are omitted here.

CROSS-HELICITY EFFECT

We examine why the production term $P_{\gamma z}$ has a positive gradient in the channel core region. The mean vorticity $\Omega_z = -(\partial U_x/\partial y)$ has a positive gradient due to the external force f_x. We then need to explain the origin of positive W_{yy} observed in Figure 7. The transport equation for the cross helicity $W_{xx}(=\langle u'_x b'_x \rangle)$ and W_{yy} are given by

$$\frac{\partial W_{xx}}{\partial t} = p_u + p_b + \Pi_{wxx} + D_{wxx} - \varepsilon_{wxx} \tag{18}$$

$$P_u = \langle u'_x b'_y - u'_y b'_x \rangle \frac{\partial U_x}{\partial y} \tag{19a}$$

$$P_b = -\langle u'_x u'_y - b'_x b'_y \rangle \frac{\partial B_x}{\partial y} \tag{19b}$$

$$\Pi_{wxx} = \langle p'_M \frac{\partial b'_x}{\partial x} \rangle \tag{19c}$$

$$\frac{\partial W_{yy}}{\partial t} = \Pi_{wyy} + D_{wyy} - \varepsilon_{wyy} \tag{20}$$

$$\Pi_{wyy} = \langle p'_M \frac{\partial b'_y}{\partial y} \rangle \tag{21}$$

Here, P_u and P_b are the production terms of W_{xx} equation that are related to the mean field. $\Pi_{w\alpha\alpha}$ is the pressure-magnetic-strain term, and the definitions of the dissipation term $-\varepsilon_{wxx}$ and $-\varepsilon_{wyy}$, and the diffusion term D_{wxx} and D_{wyy} are omitted here. Figure 9 shows the terms on the RHS of (18). The production term P_u has negative values at all y locations whereas the production term P_b has positive values at all y locations. It implies that P_u decreases the turbulent cross helicity whereas P_b generates the turbulent cross helicity W_{xx}. The pressure-magnetic-strain term Π_{wxx} has negative values at all y locations. Because the sum of the pressure-magnetic-strain terms $\Pi_{wxx} + \Pi_{wyy} + \Pi_{wzz}$ vanishes due to the magnetic solenoidality, negative values of Π_{wxx} represent the cross helicity is transferred from W_{xx} to the other components.

Figure 10 shows the terms on the RHS of (20). The positive W_{yy} is obtained due to the positive value of the pressure-magnetic-strain term Π_{wyy}. It represents that the cross helicity is transferred from W_{xx} to W_{yy}, and as a result, the positive W_{yy} was obtained in the channel.

Figure 11 illustrates the mechanism of the cross-helicity dynamo in the present flow. Once the positive B_x is generated in the channel, its gradient $\partial B_x/\partial y$ and the negative of the MHD Reynolds stress $-\langle u'_x u'_y - b'_x b'_y \rangle$ generates the positive W_{xx} by the production term $P_b = -\langle u'_x u'_y - b'_x b'_y \rangle (\partial B_x/\partial y)$. Then the cross helicity is transferred from W_{xx} to W_{yy} by the pressure-magnetic-strain term. Finally, W_{yy} and Ω_z produce the turbulent electromotive force E_{Mz}, which generates the positive B_x, forming a positive feedback loop.

PUMPING EFFECT

The production term P_{pz} related to the pumping effect plays a role of the dynamo effect that increases the mean magnetic field B_x over time in the core region. However, the physical mechanism behind this effect is not clear. In this section, we will investigate the pumping dynamo effect from the physical viewpoint of the pumping velocity $\boldsymbol{u}_p$. The pumping velocity plays a role of the mean velocity field in the induction equation for the mean magnetic field; that is, convection and bending of the magnetic field lines. The production term $P_{pz} = \left(\partial K_{Ryy}/\partial y\right) B_x$ related to the pumping effect can be expressed by the form $P_{pz} = \left\{\left(-\boldsymbol{\nabla} K_{Ryy}\right) \times \boldsymbol{B}\right\}_z$. According to the pumping effect term $\boldsymbol{u}_p \times \boldsymbol{B}$ in (7), in the present simulation of the channel flow, the pumping velocity is in the y direction, and u_{py} is proportional to $-\partial K_{Ryy}/\partial y$ and shows convection effect on the mean magnetic field B_x.

Figures 12 and 13 show the profiles of the turbulent residual energy K_{Ryy} and the negative of its gradient $-\partial K_{Ryy}/\partial y$, respectively. The turbulent residual energy K_{Ryy} has positive values with peak in the near-wall region and gradually decreases towards the channel center, which leads to the pumping velocity towards the channel center in the core region at $-0.75 < y < 0.75$ as shown in Figure 13. In Figure 14, a schematic is presented to illustrate the pumping effect in the core region from the physical viewpoint of the pumping velocity. In the core region at $-0.75 < y < 0.75$, the pumping velocity is directed towards the channel center. The effect of the pumping velocity is that more magnetic field lines are pumped to the channel center and the density of the magnetic field lines increases. It represents the mean magnetic field B_x is increased in this core region, against the diffusion effect which reduces the curvature of the mean magnetic field. Therefore, the pumping effect plays a role of dynamo effect in the core region.

CONCLUSIONS

A DNS of MHD turbulent channel flow was carried out to investigate turbulent dynamo effect. A DNS data of non-MHD channel flow was used as the initial velocity field whereas a random seed with zero mean was used to set the initial magnetic field. Time history of the volume-averaged magnetic field showed that a positive magnetic field was generated and sustained. To investigate the mechanism of the magnetic field generation, we obtained the mean fields and the statistical quantities by averaging over the x-z plane and over the time period of steady state. First, we pointed out the relationship between the production terms of the transport equation for the turbulent electromotive force and its model expression. Next, we examined the induction equation for the mean magnetic field. It was shown that the turbulent electromotive force contributes to the magnetic field generation against the Ohmic term. We further evaluated the production terms of the turbulent electromotive force to analyze the effect of the related dynamo terms.

It was shown that among the production terms, the cross-helicity effect term generates the mean magnetic field against the turbulent diffusivity effect and plays a role of the dominant dynamo effect in the channel flow. The transport equation for the cross helicity was examined to investigate the generation of the positive cross helicity W_{yy}. It implies that the positive cross helicity was first generated in the W_{xx}, then transferred to W_{yy}. Therefore, the mechanism of the cross-helicity effect in the present channel flow can be understood considering the following loop. Once the positive B_x is generated in the channel, its gradient $\partial B_x/\partial y$ and the negative of the MHD Reynolds stress $-\langle u'_x u'_y - b'_x b'_y \rangle$ generate the positive W_{xx} by the production term $P_b = -\langle u'_x u'_y - b'_x b'_y \rangle (\partial B_x/\partial y)$. Then the cross helicity is transferred from W_{xx} to W_{yy} by the pressure-magnetic-strain term. Finally, W_{yy} and Ω_z produce the turbulent electromotive force E_{M_z}, which generates the positive B_x. By this positive feedback loop, the mean magnetic field was generated and sustained in the present channel flow.

In addition to the cross-helicity effect, the role of the pumping effect is also examined. In the core region, the pumping effect also plays a role of the dynamo effect that increases the mean magnetic field. We recognized that the pumping effect corresponds to a convective transport caused by the pumping velocity which is proportional to the minus the gradient of the turbulent residual energy K_{Ryy}. Pumping the magnetic field lines towards the channel center makes the density of the magnetic field lines increase and increases the mean magnetic field in the core region of the channel.

REFERENCES

Hamba, F., and Tsuchiya, M., 2010, "Cross-Helicity Dynamo Effect in Magnetohydrodynamic Turbulent Channel Flow", *Physics of Plasmas*, Vol. 17, 012301.

Krause, F., and Radler, K. H., 1980, "Mean-Field Magnetohydrodynamics and Dynamo Theory", Pergamon Press.

Moffatt, H. K., 1978, "Field Generation in Electrically Conducting Fluids", Cambridge University Press.

Parker, E. N., 1979, "Cosmical Magnetic Fields", Oxford University Press.

Yokoi, N., 2023, "Unappreciated Cross-Helicity Effects in Plasma Physics" Anti-Diffusion Effects in Dynamo and Momentum Transport", *Reviews of Modern Plasa Physics*, Vol. 7, 33

Yoshizawa, A., and Hamba, F., 1988, "A Turbulent Dynamo Model for the Reversed Field Pinches of Plasma", *The Physics of Fluids*, Vol. 31, pp. 2276-2284.

Yoshizawa, A., 1990, "Self-Consistent Turbulent Dynamo Modeling of Reversed Field Pinches and Planetary Magnetic Fields", *Physics of Fluids B*, Vol. 2, pp. 1589-1600.

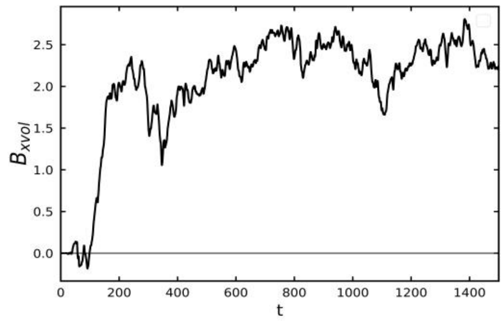

Figure 1. Time history of volume-averaged magnetic field B_{xvol}.

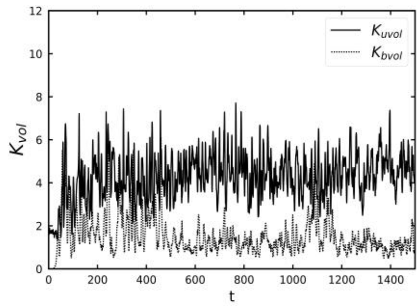

Figure 2. Time history of volume-averaged turbulent kinetic and magnetic energy K_{uvol} and K_{bvol}.

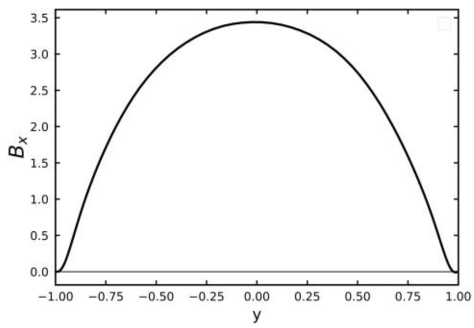

Figure 3. Profile of the mean magnetic field B_x.

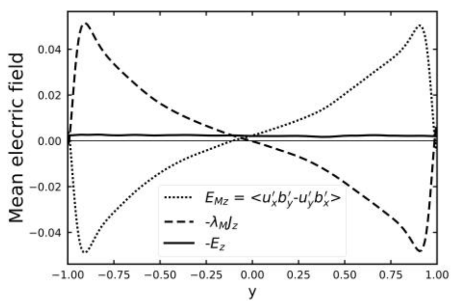

Figure 4. Profiles of mean electric field $-E_z$ and its components: the turbulent electromotive force E_{Mz} and the Ohmic term $-\lambda_M J_z$.

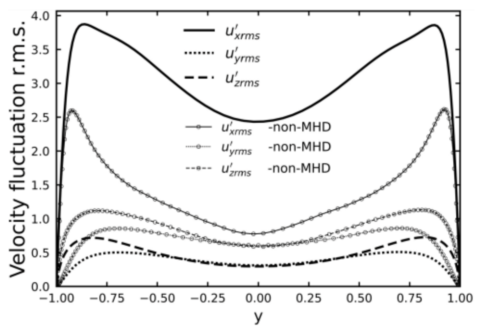

Figure 5. Profiles of three components of RMS of the velocity fluctuations in the present MHD flow and non-MHD case.

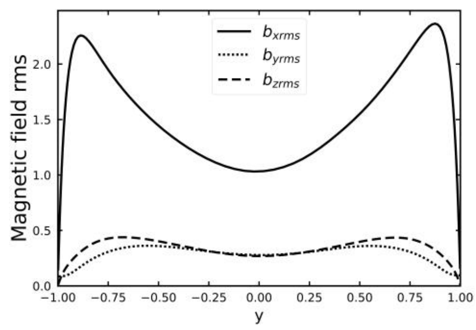

Figure 6. Profiles of three components of RMS of the magnetic field fluctuations.

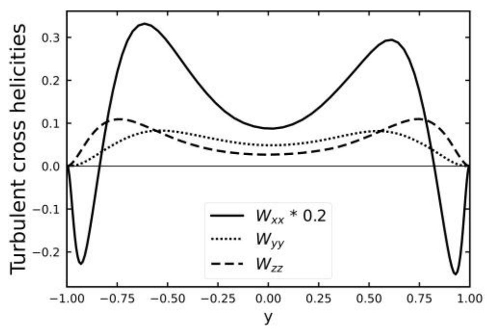

Figure 7. Profiles of three components of turbulent cross helicity.

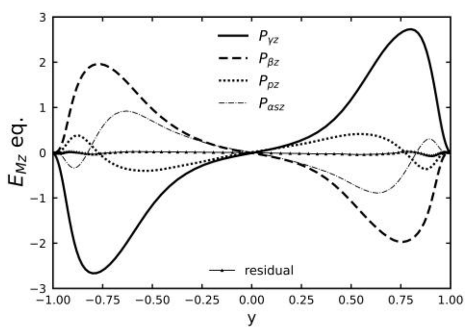

Figure 8. Profiles of production terms of E_{Mz} equation.

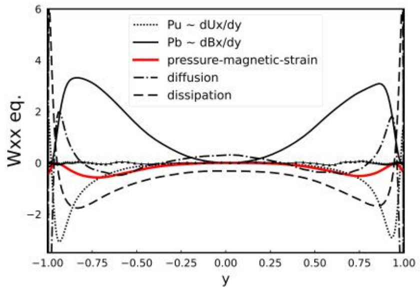

Figure 9. Balance of terms in the transport equation for the turbulent cross helicity W_{xx} given by (18).

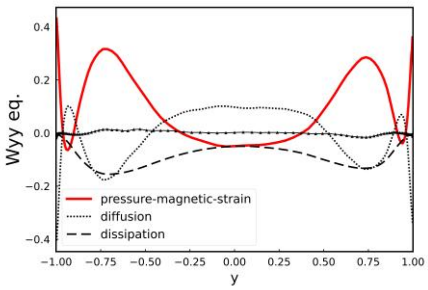

Figure 10. Balance of terms in the transport equation for the turbulent cross helicity W_{yy} given by (20).

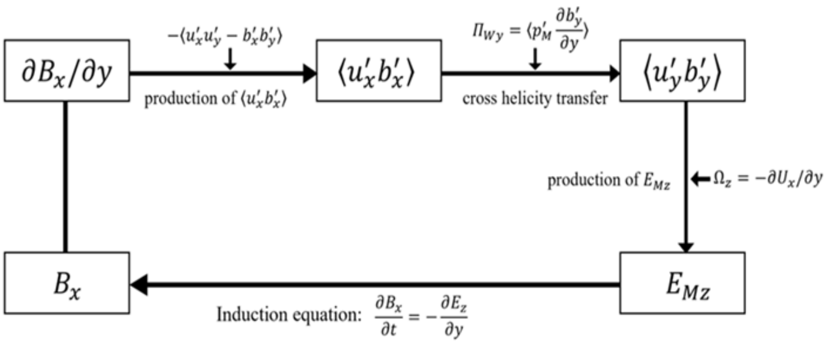

Figure 11. The mechanism of the cross-helicity effect in the present channel flow.

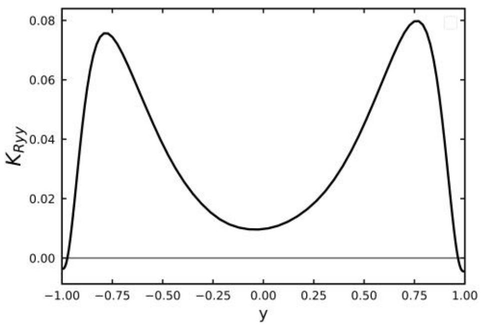

Figure 12. Profile of turbulent residual energy K_{Ryy}.

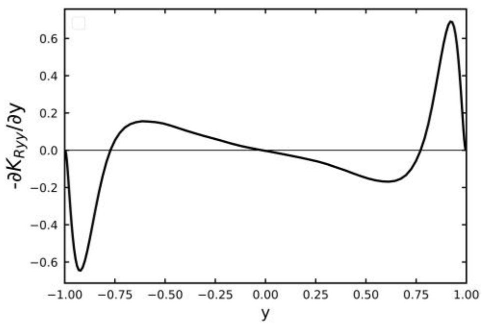

Figure 13. Profile of the quantity $-\partial K_{Ryy}/\partial y$.

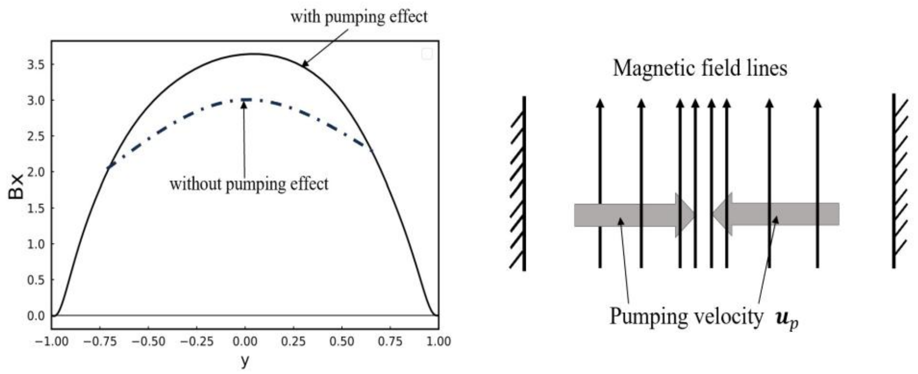

Figure 14. A schematic of pumping effect in the present channel flow.